German Journal of Veterinary Research

eISSN:2703-1322

Research article

Comparative effect of dose escalation of nanocapsulated ivermectin against mange in rabbits

Azza M. M. Abdelmoteleb[1], Dalia M. A.Elmasry[2*], Fatma H. Amro[3] and Reham A. A.Mahmoud[1]

[1] Chemistry, Toxicology and Feed Deficiency Department, Animal Health Research Institute, Agricultural Research Center, Giza 12619, Egypt
[2] Nanomaterials Research and Synthesis Unit, Animal Health Research Institute, Agricultural Research Center, Giza 12619, Egypt
[3] Reference Laboratory of Veterinary Control on Poultry Production (RLQP), Animal Health Research Institute, Agricultural Research Center, Giza 12619, Egypt

Article History:
Received: 25-Apr-2022
Accepted: 10-Jul-2022
***Corresponding author:**
Dalia M.A.Elmasry
dr_daliaelmasry@ahri.gov.eg

Abstract

The present study aimed to investigate the effects of nano-capsulated ivermectin on the liver and kidney function and oxidative status in mite infested-rabbits, compared to ivermectin. Additionally, the ivermectin residue profile in adipose tissue, liver, muscle, and kidney was evaluated. For this purpose, nano-capsulated ivermectin was prepared and characterized using high-resolution transmission electron microscopy (HRTEM) and cytotoxicity assay on Vero cells. To assess the effect of dose escalation of nano-capsulated ivermectin, one-hundred naturally mite-infested male rabbits were divided into four groups (G1-G4; n=25). Rabbits kept in G1 were left untreated (positive control), while rabbits kept in G2 and G3 received subcutaneously 200 and 400 μg/kg body weight ivermectin, respectively, at zero-day and repeated after two weeks of the first injection. Rabbits in G4 were treated with 200 μg nano-capsulated ivermectin at zero day as a single dose. Additionally, twenty-five healthy male rabbits (G0) were used as a negative control. The efficacy was assessed based on clinical manifestations, liver and kidney function, and oxidative stress parameters. Ivermectin residues were measured in fat, liver, muscle, and kidney using high-performance liquid chromatography (HPLC). Results showed that the size of the nano-capsulated ivermectin was 35.4 nm with a narrow size distribution of 0.578 polydispersity indexes. A significant improvement in liver and kidney functions ($P<0.05$) was observed in G4 received nano-capsulated ivermectin compared with G1, G2, and G3. Moreover, the oxidative stress marker malondialdehyde (MDA) showed significantly lower levels ($P<0.05$) in rabbits kept in G4. The nano-capsulated ivermectin treatment had the lowest ivermectin residues in edible tissues with the shortest withdrawal duration (14 days) below the maximum residue limits. The study concluded that nano-capsulated ivermectin is the recommended antiparasitic against mites in rabbits.

Keywords: Ivermectin nano-capsulated, Liver and kidney function, Mite, Oxidative status, Maximum residue limits

Citation: Abdelmoteleb, A. M. M., Elmasry, Dalia M. A., Amro, F. H., Mahmoud, R. A. A. 2022. Comparative effect of dose escalation of nanocapsulated ivermectin against mange in rabbits. Ger. J. Vet. Res. 2 (4): 8-15. https://doi.org/10.51585/gjvr.2022.4.0043

Introduction

Psoroptes cuniculi (*P. cuniculi*) and *Sarcoptes scabiei* (*S. scabiei*) var. *cuniculi* are the most common ectoparasitic mites in rabbits and impose a public health hazard (Nong et al., 2013; Kachhawa et al., 2013). *P. cuniculi* infestation in rabbits causes intense pruritus, serious scabs, and exudations in the external acoustic meatus (Nong et al., 2013; Shang et al., 2014). However, *S. scabiei* infestation leads to dermatitis, hair loss, pruritic scabs, and skin thickening. Mite infestation in Egyptian rabbit farms causes significant economic losses due to high mortality rates of newly born and high morbidity rates in adults (El-Ashram et al., 2020). Additionally, mite infestation in rabbits predisposes to coccidiosis infestation (Darzi et al., 2007; Seddiek et al., 2013; El-Ashram et al., 2020).

Till now, the acaricides of choice against mites in rabbits is ivermectin (Guo et al., 2018). However, drug residues and the potential for drug resistance development are a great disadvantage of ivermectin use. Ivermectin residues could be detected in kidneys for up to three days, skeletal muscles, or liver for up

to seven days, and skin and fat up to 15 days post-treatment threatening human consumers for these edible tissues with toxicity and parasite resistance (Omura and Crump, 2014). This highlights the urgent need to improve ivermectin or develop alternative treatments for *S. scabiei* and *P. cuniculi* infections.

Nanotechnology is one of the potential ways to minimize these adverse effects (Guo et al., 2018; Telia et al., 2017; Sala et al., 2018). Nano-drug delivery systems have been proposed for antiparasitic therapy delivery to raise bioavailability, sustained release, and intracellular penetrability (Gamboa et al., 2016). Therefore, the current work aimed to evaluate ivermectin nanoparticles in naturally mite-infested rabbits.

Material and methods

Preparation and characterization of nano-capsulated ivermectin

The nano-capsulated ivermectin was prepared according to Patel et al. (2018). Briefly, 30 mg/mL pure ivermectin (Animal Health Research Institute, Giza, Egypt), 4 mL span 80 (Merck, Darmstadt, Germany), and 0.3 mL/mL tween 80 (Merck, Darmstadt, Germany) and 6.17 mL/mL soybean oil (National Research center, Giza, Egypt) were mixed for 30 min in a homogeneous blender 1500 watt, and then distilled water was slowly added up to 100 mL to the mixed oil phase . High-resolution transmission electron microscopy (HRTEM) monitoring is carried out using a JEM 1400F HRTEM at a beam energy of 300 keV to characterize the ivermectin nanoemulsion and measure electrical conductivity, zeta potential (surface charge), and both size droplet and distribution (polydispersity indexes PDI) of nanoemulsion using Zetasizer Malvern Instrument (Corp, Malvern, UK).

Cytotoxicity assay of nano-capsulated ivermectin

Vero cells donated from Nawah Scientific Inc. for cell culture (Cairo, Egypt) were grown in Dulbecco's Modified Eagle Medium (DMEM, ThermoFisher GmbH, UK) media supplemented with 100 unit/mL penicillin, 100 mg/mL streptomycin, and 10% heat-inactivated fetal bovine serum in a humidified in a 5% (v/v) CO_2 incubator at 37°C. Cell viability was determined using sulforhodamine B (SRB) at various concentrations (0.01, 0.1, 1, 10, and 100 μg/mL), as described by Ammerman et al. (2008). Briefly, aliquots of a 100 mL cell suspension (containing $5x10^3$ cells) were incubated in a full medium in 96-well plates for 24 hours.

The cells were then given a second aliquot of 100 mL of medium containing encapsulated ivermectin in concentrations ranging from (0.01, 0.1, 1, 10, and 100 g/mL). After 72 hours, cells were fixed by removing the medium and adding 150 mL of 10% Trichloroacetic acid (TCA) (Merck, Darmstadt, Germany), and incubating for an hour at 4°C. Cells were washed five times with distilled water after the TCA solution was removed. Aliquots of a 70 mL SRB solution (Merck, Darmstadt, Germany) at 0.4 percent by volume were then added and incubated for 10 minutes at room temperature in a dark environment.

Assessment of the efficacy of nano-capsulated ivermectin

Animal ethics

The Institutional Animal Care and Use Committee (ARC-IACUC) at Agricultural Research Center is organized and operated according to the World Organization for Animal Health (OIE) and the Eighth Edition of the Guide for the Care and Use of Laboratory Animal (2011). The ethical committee approved sample collection from 9/01/2021 till 1/05/2021 via an authorized veterinarian applying minimum constrain to the animals and using approval sample collection methods. (ARC-AH-21/15).

Experimental design

A total of one-hundred naturally mite-infested male rabbits with an average body weight of 1700±100 g were obtained from a farm and divided into four groups (G1-G4). Mange infestation was identified based on lesions and confirmed microscopically by taking skin scraping samples smoothly with a scalpel blade dipped in mineral oil to examine the mobility and morphology according to Bowman (2021). Additionally, twenty-five healthy male rabbits and mange free were used as a negative control.

Rabbits kept in G1 (n=25) were untreated (positive control), while rabbits kept in G2 and G3 received subcutaneously 200 and 400 μg/kg body weight ivermectin, the same dose was repeated after 2 weeks. Rabbits kept in G4 were treated with 200 μg/kg body weight nano-capsulated ivermectin as a single dose (Lu et al., 2018). All rabbits were free to access to a commercial pelleted diet and water. Blood samples were obtained two weeks post-treatment for assessment of kidney and liver function parameters and antioxidant indicators by a calorimetric method using standard kits (Bio-diagnostic, Cairo, Egypt) according to the manufacturer. Seven days post the 2nd dose of treatment, five rabbits from each group were slain to collect fat, liver, muscle, and kidney samples for assessment of ivermectin residue using high-performance liquid chromatography (HPLC) device. The procedures were repeated weekly for another three times.

Biochemical tests

Liver and kidney function tests

Serum aspartate aminotransferase activity (AST) was determined using commercial kits (Biodiagnostic, Giza, Egypt). Serum alanine aminotransferase activity (ALT) was determined calorimetrically using a TECO kit, (TECO Diagnostic, California, USA), serum urea was determined enzymatically using commercial kits (BioMed-Urea/BUN-(UV), Cairo, Egypt) and serum creatinine was determined calorimetrically using commercial kits (Biodiagnostics, Giza, Egypt).

Antioxidant and oxidative stress biomarker tests

Glutathione-S-Transferase (GST), superoxide dismutase (SOD), malondialdehyde (MDA), and lipid peroxidase were determined using commercial kits (Biodiagnostic, Giza, Egypt).

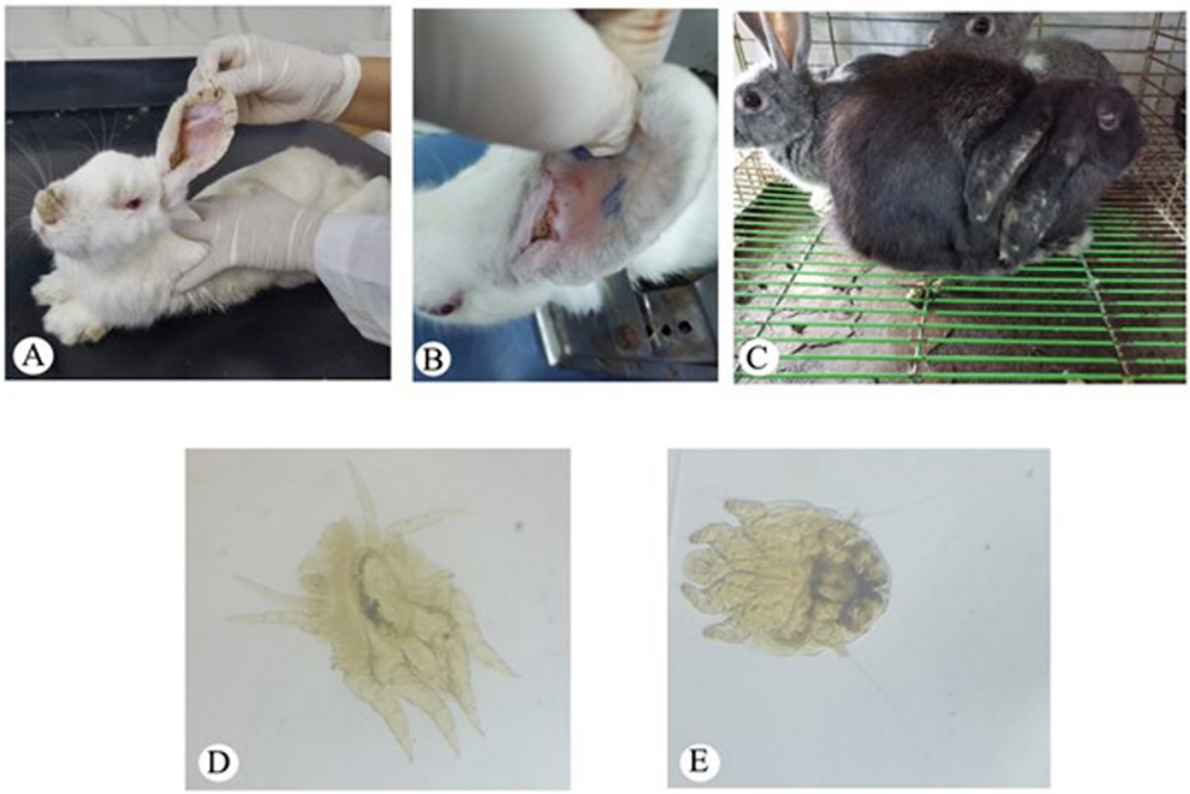

Figure 1: Clinical ear lesions caused by *Psoroptes cuniculi* (A) and crustaceous lesions on the body caused by *Sarcoptes scabie* (B, C) before treatment. *Psoroptes cuniculi* appeared as oval-shaped with well-developed legs that project beyond the body margin (D). Adult *Sarcoptes scabiei* appeared as spherical, ventrally flattened and dorsally convex tortoise-like bodies and multiple cuticular spines (E).

Estimation of ivermectin residue in rabbit tissue

Stock standard solution of ivermectin was formulated at a 1 mg/mL (1000 ppm) concentration in methanol and kept in amber glass at 4°C till use. It was diluted with methanol to obtain the fortification solution at a concentration of 10 ppm, which should be freshly prepared. The calibration curve was created by fortifying blank rabbit tissues with various volumes of fortification solution to yield a concentration range of 2-500 ppb (calibration samples) and spike blank tissues to prepare quality control (QC) samples at 50, 100, and 200 ppb for fat and liver, at 15, 30 and 60 ppb for kidneys and muscle. The standards were injected three times onto HPLC. The analysis of ivermectin was performed by HPLC with solid-phase extraction (SPE) (Strata, C18, 250 mg, 3mL) and fluorescence detection following the methodology previously defined by Mestorino et al. (2017) with minor adjustments to increase accuracy and sensitivity.

One gram of minced fat, liver, muscles, and kidney was homogenized in 2 mL of acetonitrile for 10 min and sonicated for 10 min, then centrifuged at 4°C at 2000 ×g for 2 min. The supernatant was transferred to another polypropylene-containing tube, and the extraction was repeated. Collected supernatants were applied to SPE C18 cartridges that were preconditioned with 1 mL of methanol and then 1 mL of distilled water. All samples were loaded to the activated cartridge, washed with 1 mL of water followed by 1 mL of methanol/water (1:3, v/v), dried for 2 min with air, and eluted with 3 mL of methanol HPLC grade. The obtained eluent evaporated at 60°C using an N2 evaporator. The dry residue was dissolved in 100 μL of a mixture of N-methylimidazole solution in acetonitrile (1:1, v/v).

To initiate the derivatization, 150 μL of a solution of trifluoroacetic anhydride in acetonitrile (1:2, v/v) was added and mixed for 30 seconds. The extract was injected immediately into the HPLC system. HPLC parameters required chromatographic conditions mobile phase (acetonitrile: methanol: 2% acetic acid; 64: 32: 4), 1.5 mL/min of flow rate, 100 μL injection volume, C18 column (Agilent, 250 mm × 4.6 mm, 3.5μm), 35°C of the column and excitation at 365 nm and emission at 475 nm of fluorescence detector were using Agilent Series 1200 quaternary gradient pump, Series 1200 autosampler, Series 1200 FLD is a detector and HPLC 2D Chemistation software. The analytical method was validated according to requirements (ICH, 2015) in terms of linearity and range, intra-day & inter-day precision, recovery, limits of detection and quantification (LOD & LOQ), robustness, system suitability test (SST), and specificity was determined using QC samples.

Statistical Analysis

The obtained results are shown as the Mean ± Standard Deviation (Mean±SD) and analyzed with SPSS by using the ANOVA test (version 14.0; SPSS Inc,

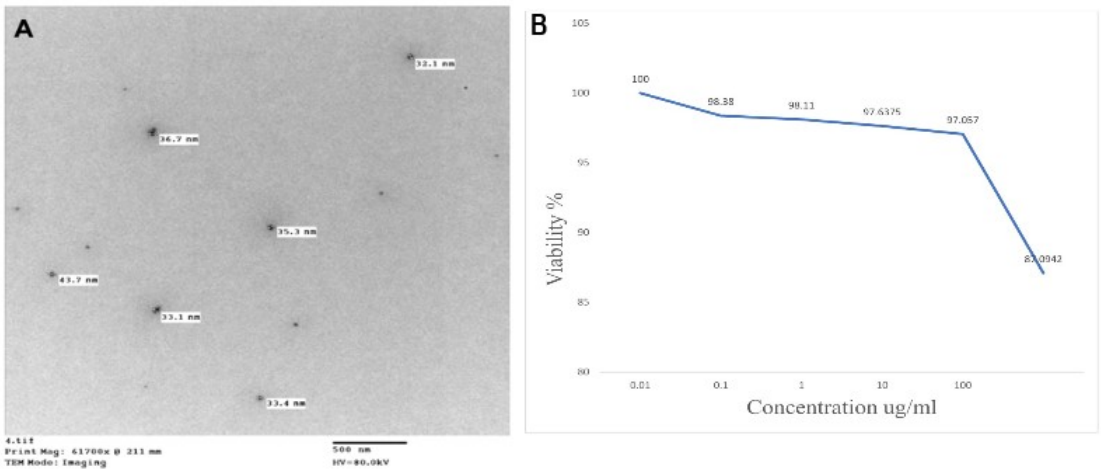

Figure 2: High-resolution transmission electron microscopy (HER-TEM) of ivermectin nanocapsulated with spherical shaped and a smooth surface, and their average particle size was 35.4 nm with a polydispersity index: 0.578 (A). Cell viability percent (%) of Vero cells treated with nanocapsulated ivermectin is 98.38, 98.11, 97.6375, 97.057, and 87.0942, respectively (B).

Chicago, Ill). The estimation of a significant difference was set at $p<0.05$ according to Neyeloff et al. (2012).

Results

Clinical and microscopical examination of mange infestation in rabbits

The microscopic examination revealed *P. cuniculi* from the ear lesions (Figure 1A,B&D) and *S. scabiei* from the dorsal surface lesions of the body (Figure 1C&E). Healthy rabbits were proved to be devoid of ectoparasites by microscopic examination of the skin scraping and used as a negative control.

Characterization of nano-capsulated ivermectin

The nanodroplet characterization of ivermectin nanocapsulated was primarily determined by HRTEM. The nano-capsulated size was 35.4 nm with distribution in narrow size (polydispersity index: 0.578), indicating that homogeneity can be achieved (Figure 2A). The zeta potential is an indicator of stable suspensions that are commonly measured using dynamic light scattering (DLS) and had a -4.33± 4.56 mV, the viscosity 0.08872 (cp), and conductivity of 0.0258ms/cm.

Cytotoxicity assay

After three days of inoculation with nano-capsulated ivermectin at different concentrations (0.01, 0.1, 1, 10, 100 μg /ml), cell viability percent was 98.38, 98.11, 97.6375, 97.057, and 87.0942, respectively, measured by SRB. and IC50= 100 μg/mL which based on the cell viability results (Figure 2B), the 50% inhibition concentration (IC50) was calculated using linear interpolation (Wu et al., 2018) as shown in (Figure 3).

Assessment of the efficacy of nano-capsulated ivermectin

The initial antiparasitic dosage was 0.58 mL for each rabbit (400 μg nano-capsulated ivermectin/kg rabbit), which resulted in rabbit mortality within seven days. Therfore, we used 0.58 mL containing 200 μg nano-capsulated ivermectin/kg rabbit which was safe for use in rabbits as indicated by safety (Data not shown).

Biochemical analyses

In the present study, ALT, AST, serum urea, and creatinine elevation were significantly lower in ivermectin treated groups than the positive control group ($P<0.05$), indicating that ivermectin treatment improved liver and kidney function. However, the most improvement was obtained in the nano-capsulated ivermectin treated group as shown in Table 1.

The oxidative stress status was assessed in all infested rabbits as detected by increased oxidative metabolites (MDA) and decreased antioxidant enzymes (SOD & GST). The treatment groups showed higher significantly different values ($P<0.05$) than the positive control group indicating that ivermectin treatment ameliorated oxidative processes. The most positive action was obtained in the group that received nano-capsulated ivermectin, as shown in Table 2.

Ivermectin tissue residues in treated rabbits

The assay was validated and verified according to ICH (2015); USP (2019). The obtained results were summarized in Table 3 showing good linearity within a range (2–500 μg/kg) in different matrices with a correlation coefficient of >0.99. This method exhibits high accuracy and recovery (87-101%), good precision, and SST results within acceptable criteria.

Drug residues study revealed that the highest concentrations of ivermectin were found in adipose tissue than in other edible tissues. The residue in both tested fat and liver was greater than that in tested kidneys and muscles, as shown in Table 3. Ivermectin was identified in high concentration on the 14^{th} day, then decreased and outstanding stable on the 28^{th} day post-treatment. However, it was clear that all over the examined tissue samples among different treated groups, the nano-capsulated ivermectin treated group achieved the lowest ivermectin residues, as shown in Table 4. Maximum residue limits (MRLs) of ivermectin were estimated in fat and liver as 100 ng/g and in kidney and muscle as 30 ng/g, as shown in Figure 3.

Table 1: Levels of urea, creatinine, alanine, and aspartate aminotransferase enzymes (ALT & AST) expressed as Mean±SD in rabbits of different treatment groups.

Paramaters	Negative control	Positive control	Mange infested and treated groups*		
			Ivermectin 200 μg/kg (G2)	Ivermectin 400 μg/kg (G3)	Nano-capsulated ivermectin 200 μg/kg (G4)
Urea (mg/dL)	32.21±1.15[d]	55.33±1.2[a]	43.66±1.86[c]	49.1±0.58[b]	43.21±1.15[c]
Creatinine (mg/dL)	0.69±0.01[c]	1.14±1.09[a]	0.78±0.75[c]	0.87±0.84[b]	0.63±0.59[c]
ALT (U/L)	6.31±0.58[c]	13.22±0.58[a]	6.41±0.58[c]	9.12±0.58[b]	5.21±0.58[c]
AST (U/L)	6.33±0.33[b]	12.67±0.84[a]	7.41±0.86[b]	10.67±0.68[a]	7.66±0.78[b]

* Values in raw with different small letters in each row were significantly different at P<0.05.

Table 2: Superoxide dismutase (SOD), glutathione-S-transferase (GST), and malonaldehyde (MDA) in control and treated rabbit groups.

Paramaters	Negative control	Positive control	Mange infested and treated groups*		
			Ivermectin 200 μg/kg (G2)	Ivermectin 400 μg/kg (G3)	Nano-capsulated ivermectin 200 μg/kg (G4)
SOD (U/mL)	22.88±1.80[a]	13.55±1.22[d]	19.05±1.51[b]	16.15±.99[c]	19.89±1.43[b]
GST (U/ml)	67.73±4.66[a]	50.38±2.46[d]	62.87±3.06[b]	58.53±3.41[c]	61.63±4.66[b]
MDA(nmol/ml)	5.1±0.22[c]	10.95±0.25[a]	6.00±0.64[b]	8.2±0.53[b]	3.95±0.15[c]

* Values in raw with different small letters in each row were significantly different at P<0.05.

Table 3: Validation sheet of ivermectin in different rabbit tissues by high-performance liquid chromatography (HPLC).

Parameter		Adipose tissue	Liver	Muscle	Kidney	Acceptance criteria
Retention time				12.161		-
Range (ppb)				2-500 ppb		-
Correlation coefficient		0.99954	0.99958	0.99994	0.99994	>0.99
LOD (ppb)		0.48	0.19	0.11	0.26	-
LOQ (ppb)		1.5	0.57	0.33	0.77	-
Recovery (%)		87-92	89-95	92-101	92-98	85- 115
Intra-day precision (CV%)		0.72	0.32	0.2	0.3	≤1
Inter-day precision (CV%)		1.3	0.42	0.31	0.31	≤2
Pooled robustness (CV%)		3.8	2.4	2.5	3.1	≤6
System suitability test	Tailing factor	1.08±0.01	1.03±0.01	1.02±0.01	1.02±0.01	≤2
	Symmetry	0.91±0.01	0.9±0.01	0.93±0.01	0.91±0.01	<1
	Theoretical plate	8051±11	8670±42	8850±25	8221±21	>2000

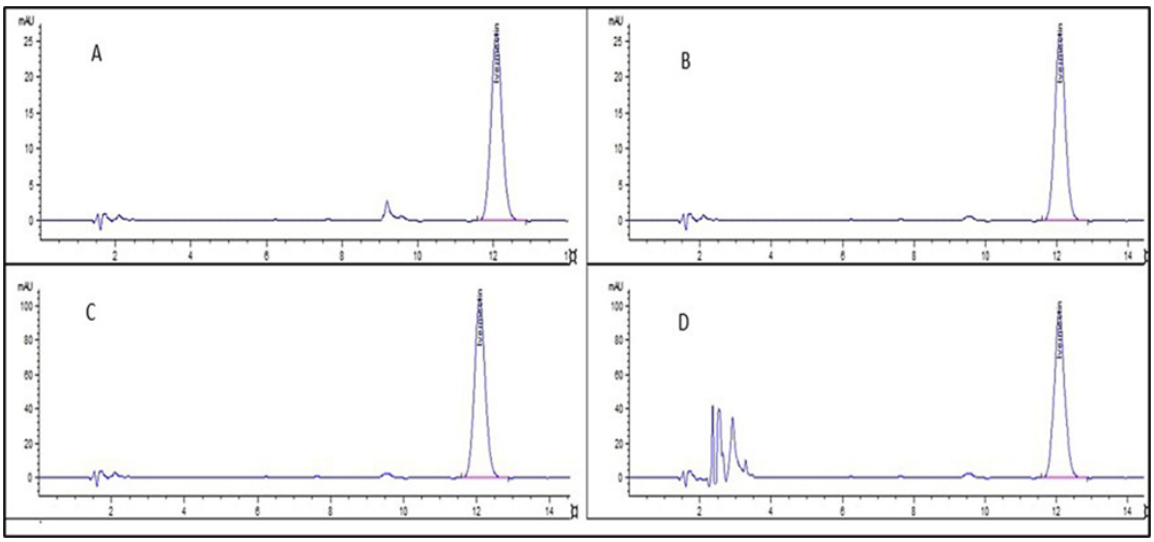

Figure 3: Chromatogram of ivermectin in the kidney at 30 ppb concentration (A), in the liver at 100 ppb concentration (B), in the muscles at 30 ppb concentration (C), and in adipose tissues at 100 ppb concentration (D).

Table 4: Validation sheet of ivermectin in different rabbit tissues by high-performance liquid chromatography (HPLC) expressed as Mean±SD.

Parameters	Groups	Days post treatment*				MRL (ppb)
		7	14	21	28	
Fat	Nano-capsulated ivermectin	125.2±19.6^{c}	52.6±5.2^{c}	19±2.5^{c}	4.8±0.4^{c}	100
	200 μg/kg ivermectin	206± 12.9^{b}	72.5±3.4^{b}	26.3±1.8^{b}	6.3±0.3^{b}	
	400 μg/kg ivermectin	250.6±12.3^{a}	87.6±5.4^{a}	36.2±2.2^{a}	9.1±0.4^{a}	
Liver	Nano-capsulated ivermectin	98.6±12.3^{c}	47±4.6^{c}	14.8±1.6^{bc}	4.2±0.3^{bc}	
	200 μg/kg ivermectin	129.1±8.1^{b}	61.6±3.1^{b}	16.6±0.1^{b}	4.6±0.2^{b}	
	400 μg/kg ivermectin	160.3±10^{a}	73.8±3.6^{a}	23.7±1.4^{a}	6.3±0.3^{a}	
Muscle	Nano-capsulated ivermectin	37.7± 4^{bc}	18.5±1.5^{bc}	4.8±0.5^{bc}	2.1±0.1^{bc}	30
	200 μg/kg ivermectin	42.1±2.7^{b}	20.7±1^{b}	5.3±0.3^{b}	2.3±0.1^{b}	
	400 μg/kg ivermectin	55.4±3.6^{a}	26.2±1.2^{a}	6.2±0.4^{a}	2.9±0.1^{a}	
Kidneys	Nano-capsulated ivermectin	60.8± 6.5^{bc}	28.9±2.4^{c}	6.6±0.7^{bc}	3.2±0.2^{bc}	
	200 μg/kg ivermectin	67.9±4.3^{b}	33.5±1.6^{b}	7.3±0.4^{b}	3.6±0.15^{b}	
	400 μg/kg ivermectin	87.4±5.6^{a}	41.3±2^{a}	9.3±0.6^{a}	4.7± 0.2^{a}	

*Values with different small letters in each column of different organs were significantly different at P<0.05.

Discussion

Nanoparticles have been proposed for antiparasitic therapy delivery to raise medicines' bioavailability, sustained release, and intracellular penetrability. The drug immobilization on or into nanoparticles is an effective method for increasing effectiveness and minimizing negative effects (Gamboa et al., 2016). nano-capsulated ivermectin is a new type of lipid nanoparticle created by combining various nanocarriers that appear to be a viable drug delivery mechanism for effective administration (Jawahar et al., 2018). Nano-capsulated ivermectin was 35.4 nm with a polydispersity index of 0.578 (Figure 2A). Despite ivermectin-loading solid lipid nanoparticles having a droplet size of 270.34 nm, homogenous nanomaterial below 500 nm can penetrate the skin epithelium (Bickers and Athar, 2006). nano-capsulated ivermectin acted the viability of Vero cells (Figure 2B) was 98.38, 98.11, 97.6375, 97.057, and 87.0942 for 0.01, 0.1, 1, 10, 100, and 1000 μg/ml concentrations, respectively.

Biochemically, parasitism-induced hepatic inflammation was detected by increased ALT and AST levels and hepatocyte apoptosis (Jenkins, 2000) and interfered with kidney function as seen by increased serum urea and creatinine levels (Nishikimi et al., 1972; NRC, 1977). The dose of 400 μg/kg BW ivermectin is a toxic excretory product (Arise and Malomo, 2009; Al-Jassim et al., 2016; Metwally et al., 2018). Since nanoparticles can cross biological barriers (Zoabi et al., 2021), they protect drugs from enzyme destruction and intracellular delivery and drug accumulation (Negi et al., 2013) that lower the toxicity, and change pharmacokinetic characteristics by increasing circulation time and improving tissue distribution (Peltier et al., 2006).

The parasitic inflammatory processes stimulate macrophages and neutrophils with reactive oxygen substances, such as hydrogen peroxide and oxygen-free radicals. These oxidative processes were observed in all infested rabbits as increased levels of the MDA (Bickers and Athar, 2006; Shang et al., 2014; Abu Hafsa et al., 2021) and decreased antioxidant enzymes (SOD & GST) (Gurgoze et al., 2003; Radwan et al., 2017). Ivermectin drug is lipophilic and binds to lipoproteins, with a particular attraction to fat tissue that serves as a primary storage site (Baynes et al., 2000; Singh, 2015). Consequently, ivermectin residues were detected in adipose tissues more than in other edible tissues of treated small or large ruminants (Dusi et al., 1996; Lifschitz et al., 2000) and poultry (Mestorino et al., 2017).

Maximum residue limits (MRLs) of ivermectin are estimated in fat and liver as 100 ng/g and in kidney and muscle, which fulfill the European requirements (EMA, 2014). The high affinity of ivermectin for adipose tissue undertakes significant hepatic metabolism, primarily via hydroxylation mechanisms (Zoabi et al., 2021), and the majority of ivermectin is eliminated through feces, and the minority via urine (Al-Jassim et al., 2016). Its residue in both tested fat and liver was greater than that in tested kidneys and muscles (Table 4). It was documented that the systemic disposition of ivermectin lipid capsule administered by the subcutaneous route was higher compared to treatment with a commercial formulation ($p<0.05$) with an encapsulation rate higher than 90% constant (Gamboa et al., 2016).

Conclusion

Using nano-capsulated ivermectin as an antiparasitic to treat mange-infested rabbits did not impair kidney and liver function and had antioxidant activity compared with commercial routes. Moreover, ivermectin nano-capsulated residues in edible tissues with a short withdrawal period are considered safe for consumption.

Article Information

Acknowledgments. We would like to thank Sahar Elwan Rizk Saba, Parasitology Department, Animal Health Research, Institute, Dokki, Giza for help in the isolation and identification of mites in experimental rabbits. The authors especially thank with appreciate Prof. Dr. Abd El-Hafeez M. M. at AHRI, Assiut Laboratory for assisting in the scientific review of the research.

Funding. This research received no funds.

Conflict of Interest. The authors have no conflict of interest to declare.

References

Abu Hafsa, S.H., Senbill, H., Basyony, M.M., Hassan, A.A., 2021. Amelioration of sarcoptic mange-induced oxidative stress and growth performance in ivermectin-treated growing rabbits using turmeric extract supplementation. Animals 11. 10.3390/ani11102984.

Al-Jassim, K.B., Jawad, A.A.H., Al-Masoudi, E.A., Majeed, S.K., 2016. Histopathological and biochemical effects of ivermectin on kidney functions, lung and the ameliorative effects of vitamin C in rabbits (*Lupus cuniculus*). Basrah Journal of Veterinary Research 14, 110–124. URL: https://basjvet.org/uplodes/pdf/1588976950.pdf.

Ammerman, N.C., Beier-Sexton, M., Azad, A.F., 2008. Growth and maintenance of Vero cell lines. Current Protocols in Microbiology Appendix 4, Appendix 4E. 10.1002/9780471729259.mca04es11.

Arise, R.O., Malomo, S.O., 2009. Effects of ivermectin and albendazole on some liver and kidney function indices in rats. African Journal of Biochemistry Research 3, 190–197. URL: https://academicjournals.org/journal/AJBR/article-stat/E62326811023.

Baynes, R.E., Payne, M., Martin-Jimenez, T., Abdullah, A.R., Anderson, K.L., Webb, A.I., Craigmill, A., Riviere, J.E., 2000. Extralabel use of ivermectin and moxidectin in food animals. Journal of the American Veterinary Medical Association 217, 668–671. 10.2460/javma.2000.217.668.

Bickers, D.R., Athar, M., 2006. Oxidative stress in the pathogenesis of skin disease. The Journal of Investigative Dermatology 126, 2565–2575. 10.1038/sj.jid.5700340.

Bowman, D.D., 2021. Georgis' parasitology for veterinarians. Elsevier, Cornell University, Ithaca, New York. 10.1016/C2016-0-02298-2.

Darzi, M., Mir, M., Shahardar, R.A., Pandit, B.A., 2007. Clinico-pathological, histochemical and therapeutic studies on concurrent sarcoptic and notoedric acariosis in rabbits (*Oryctolagus cuniculus*). Veterinarski Arhiv 77, 167–175.

Dusi, G., Curatolo, M., Fierro, A., Faggionato, E., 1996. Determination of the antiparasitic drug ivermectin in liver, muscle and fat tissue samples from swine, cattle, horses and sheep using HPLC with fluorescence detection. Journal of Liquid Chromatography & Related Technologies 19, 1607–1616. 10.1080/10826079608005495.

El-Ashram, S., Aboelhadid, S.M., Abdel-Kafy, E.S.M., Hashem, S.A., Mahrous, L.N., Farghly, E.M., Kamel, A.A., 2020. Investigation of pre- and post-weaning mortalities in rabbits bred in Egypt, with reference to parasitic and bacterial causes. Animals 10. 10.3390/ani10030537.

EMA, 2014. Ivermectin: All mammalian food producing species). Technical Report. European Medicines Agency.Committee for Medicinal. European public MRL assessment report (EPMAR) Products for Veterinary Use. Canary Wharf, London.

Gamboa, G.V.U., Palma, S.D., Lifschitz, A., Ballent, M., Lanusse, C., Passirani, C., Benoit, J.P., Allemandi, D.A., 2016. Ivermectin-loaded lipid nanocapsules: Toward the development of a new antiparasitic delivery system for veterinary applications. Parasitology Research 115, 1945–1953. 10.1007/s00436-016-4937-1.

Guo, D., Dou, D., Li, X., Zhang, Q., Bhutto, Z.A., Wang, L., 2018. Ivermection-loaded solid lipid nanoparticles: Preparation, characterisation, stability and transdermal behaviour. Artificial cells, Nanomedicine, and Biotechnology 46, 255–262. 10.1080/21691401.2017.1307207.

Gurgoze, S.Y., Sahin, T., Sevgili, M., Ozkutlu, Z., Ozan, S., 2003. The effect of ivermectin or doramectin treatment on

some antioxidant enzymes and the level of lipid peroxidation in sheep with natural *Sarcoptic scabie*. Van Veterinary Journal 14, 30–34. URL: https://dergipark.org.tr/en/pub/yyuvfd/issue/13747/166445.

ICH, 2015. International conference on harmonization of technical requirements for registration of pharmaceuticals for human use. URL: https://www.ich.org/.

Jawahar, N., Hingarh, P.K., Arun, R., Selvaraj, J., Anbarasan, A., S, S., G, N., 2018. Enhanced oral bioavailability of an antipsychotic drug through nanostructured lipid carriers. International Journal of Biological Macromolecules 110, 269–275. 10.1016/j.ijbiomac.2018.01.121.

Jenkins, J.R., 2000. Rabbit and ferret liver and gastrointestinal testing, in: Fudge, A.M. (Ed.), Laboratory Medicine: Avian and Exotic Pets. WB Saunders, Philadelphia, USA, pp. 291–304.

Kachhawa, J.P., Kachhawaha, S., Srivastava, M., Chahar, A., Singh, N.K., 2013. Therapeutic management of scabies in rabbits. Intas Polivet 14, 306–308.

Lifschitz, A., Virkel, G., Sallovitz, J., Sutra, J.F., Galtier, P., Alvinerie, M., Lanusse, C., 2000. Comparative distribution of ivermectin and doramectin to parasite location tissues in cattle. Veterinary Parasitology 87, 327–338. 10.1016/s0304-4017(99)00175-2.

Lu, M., Cai, Y., Yang, S., Wan, Q., Pan, B., 2018. A single subcutaneous administration of a sustained-release ivermectin suspension eliminates *Psoroptes cuniculi* infection in a rabbit farm. Drug Development and Industrial Pharmacy 44, 2000–2004. 10.1080/03639045.2018.1506474.

Mestorino, N., Buldain, D., Buchamer, A., Gortari, L., Daniele, M., Marchetti, M.L., 2017. Residue depletion of ivermectin in broiler poultry. Food additives & Contaminants. Part A, Chemistry, analysis, control, exposure & risk assessment 34, 624–631. 10.1080/19440049.2016.1278307.

Metwally, D.M., Al-Olayan, E.M., Alshalhoop, R.A., Eisa, S.A., 2018. Biomarkers as predictive tools to test the *in-vivo* antisarcoptic mange activity of propolis in naturally infested rabbits. Bioscience Reports 38. 10.1042/BSR20180874.

Negi, J.S., Chattopadhyay, P., Sharma, A.K., Ram, V., 2013. Development of solid lipid nanoparticles (SLNs) of lopinavir using hot self nano-emulsification (SNE) technique. European Journal of Pharmaceutical Sciences 48, 231–239. 10.1016/j.ejps.2012.10.022.

Neyeloff, J.L., Fuchs, S.C., Moreira, L.B., 2012. Meta-analyses and forest plots using a microsoft excel spreadsheet: Step-by-step guide focusing on descriptive data analysis. BMC Research Notes 5, 52. 10.1186/1756-0500-5-52.

Nishikimi, M., Appaji, N., Yagi, K., 1972. The occurrence of superoxide anion in the reaction of reduced phenazine methosulfate and molecular oxygen. Biochemical and Biophysical Research Communications 46, 849–854. 10.1016/s0006-291x(72)80218-3.

Nong, X., Ren, Y.J., Wang, J.H., Fang, C.L., Xie, Y., Yang, D.Y., Liu, T.F., Chen, L., Zhou, X., Gu, X.B., Zheng, W.P., Peng, X.R., Wang, S.X., Lai, S.J., Yang, G.Y., 2013. Clinical efficacy of botanical extracts from eupatorium adenophorum against the scab mite, *Psoroptes cuniculi*. Veterinary Parasitology 192, 247–252. 10.1016/j.vetpar.2012.10.005.

NRC, 1977. Nutrient requirements of rabbits, in: Nutrient Requirements of Domestic Animals. 2nd ed.. National Academy of Science, Washington, DC, USA.

Omura, S., Crump, A., 2014. Ivermectin: Panacea for resource-poor communities? Trends in Parasitology 30, 445–455. 10.1016/j.pt.2014.07.005.

Patel, V.P., Lakkad, H.A., Ashara, K.C., 2018. Formulation studies of solid self-emulsifying drug delivery system of ivermectin. Folia Medica 60, 580–593. 10.2478/folmed-2018-0024.

Peltier, S., Oger, J.M., Lagarce, F., Couet, W., Benoît, J.P., 2006. Enhanced oral paclitaxel bioavailability after administration of paclitaxel-loaded lipid nanocapsules. Pharmaceutical Research 23, 1243–1250. 10.1007/s11095-006-0022-2.

Radwan, M.E.I., Samir, R.E., Mohamed, A.E.M., 2017. Biochemical changes investigated by Psoroptic mange infestation in buffaloes. Journal of Mind and Medical Sciences 8, 20–24. 10.14303/jmms.2017.015.

Sala, M., Diab, R., Elaissari, A., Fessi, H., 2018. Lipid nanocarriers as skin drug delivery systems: Properties, mechanisms of skin interactions and medical applications. International Journal of Pharmaceutics 535, 1–17. 10.1016/j.ijpharm.2017.10.046.

Seddiek, S.A., Khater, H.F., El-Shorbagy, M.M., Ali, A.M., 2013. The acaricidal efficacy of aqueous neem extract and ivermectin against `Sarcoptes scabiei` var. *cuniculi* in experimentally infested rabbits. Parasitology Research 112, 2319–2330. 10.1007/s00436-013-3395-2.

Shang, X., Wang, D., Miao, X., Wang, X., Li, J., Yang, Z., Pan, H., 2014. The oxidative status and inflammatory level of the peripheral blood of rabbits infested with *Psoroptes cuniculi*. Parasites & Vectors 7, 124. 10.1186/1756-3305-7-124.

Singh, J., 2015. International conference on harmonization of technical requirements for registration of pharmaceuticals for human use. Journal of Pharmacology & Pharmacotherapeutics 6, 185–187. 10.4103/0976-500X.162004.

Telia, Kale, R.D., Bhatt, L., 2017. Effect of nanoclay loading on zeta potential of polyester nanocomposite fibre. Indian Journal of Fibre & Textile Research 42, 125–131.

USP, 2019. Validation of compendial procedures and chromatography, in: United States Pharmacopeia. Rockville, Rockville, MD.

Wu, Y.N., Shieh, D.B., Yang, L.X., Sheu, H.S., Zheng, R., Thordarson, P., Chen, D.H., Braet, F., 2018. Characterization of iron coregold shell nanoparticles for anti-cancer treatments: Chemical and structural transformations during storage and use. Materials 11. 10.3390/ma11122572.

Zoabi, A., Touitou, E., Margulis, K., 2021. Recent advances in nanomaterials for dermal and transdermal applications. Colloids and Interfaces 5, 18. 10.3390/colloids5010018.